



Synthesis, experimental and theoretical studies on the factors influencing the pK_a values of new crown ethers containing a diarylphosphinic acid unit



Tamás Szabó^a, Gergő Dargó^{a, b}, Hajnalka Szentjóni^a, Tünde Tóth^a, Balázs Krámos^c,
 Richárd Izrael^d, Julianna Oláh^d, Tamás Németh^a, György T. Balogh^{b, **, *}, Péter Huszthy^{a, *}

^a Department of Organic Chemistry and Technology, Budapest University of Technology and Economics, H-1521 Budapest, PO Box 91, Hungary

^b Compound Profiling Laboratory, Chemical Works of Gedeon Richter Plc., H-1475, Budapest, PO Box 27, Hungary

^c Spectroscopic Research, Chemical Works of Gedeon Richter Plc., H-1475, Budapest, PO Box 27, Hungary

^d Department of Inorganic and Analytical Chemistry, Budapest University of Technology and Economics, H-1111 Budapest Szent Gellért tér 4, Hungary

ARTICLE INFO

Article history:

Received 2 September 2016

Received in revised form

3 November 2016

Accepted 14 November 2016

Available online 15 November 2016

Keywords:

Proton-ionizable crown ethers

Diarylphosphinic acids

pK_a determination

DFT, MD simulations

Acidity

ABSTRACT

Synthesis of acidic new crown ethers containing a diarylphosphinic acid unit has been accomplished. The aromatic rings of the crown ethers were substituted with *tert*-butyl and nitro groups. Nitro substitution of the crown ethers was investigated. pK_a determination of the new proton-ionizable crown ethers has been performed, showing the effect of the substituents of the aromatic rings on the acidity. An anomaly was discovered in the pK_a values and an explanation was given based on quantum mechanical calculations and molecular dynamics simulations.

© 2016 Elsevier Ltd. All rights reserved.

1. Introduction

In Nature molecular recognition is a very important phenomenon. Examples for its action are the formation of the DNA double helix and the enzyme–substrate interaction. This kind of natural phenomenon can be imitated by synthetic molecules such as crown ethers, which belong to a group of macrocycles capable of forming complexes with various ions or molecules.¹ Since the pioneering work of Charles Pedersen, who discovered the crown ethers,² many analogous macrocycles have been synthesized for versatile purposes.³ The selectivity in complex formation of crown ethers is primarily influenced by secondary interactions between the host and guest molecules. Among these the ionic interaction, which is characteristic for proton-ionizable crown ethers,⁴ plays a prominent role.

Our interest has also been focussed on crown ethers containing a monoprotic acidic moiety.^{4i-m,5} This type of proton-ionizable macrocycles can be used as cation carriers in bulk liquid membrane cells.^{4a,4c} For our studies the diarylphosphinic acid unit was chosen recently as the proton-ionizable part, because it was expected that the aromatic rings render a rigid conformation to the crown ethers, which could increase the selectivity of the complexation.^{4j,4l,4m,5}

Beside steric effects, the pK_a of the diarylphosphinic acid part can be tuned by substitution of the aromatic rings.⁶ Earlier we reported the synthesis and transport studies of enantiopure, lipophilic crown ethers containing a diarylphosphinic acid unit.^{4m,5} In that study we examined the substituted (at the aromatic rings) macrocycles, and explained the effect of substitution for the transport. We think that it is very important to know the pK_a values of these crown ethers, but the high lipophilicity of those compounds (containing decyl groups at the chiral centers) makes it difficult to determine their pK_a values in aqueous media, therefore we have synthesized the achiral analogues **1–6** (see Fig. 1), which are less lipophilic, thus it is easy to measure the proton dissociation constants by pH- and UV-pH-metric techniques in aqueous

* Corresponding author.

** Corresponding author.

E-mail addresses: gy.balogh@richter.hu (G.T. Balogh), huszthy@mail.bme.hu (P. Huszthy).

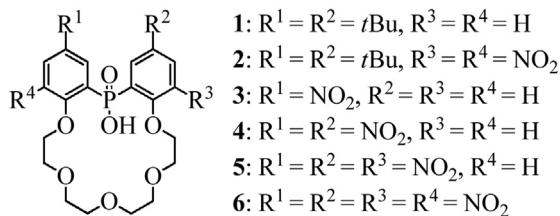


Fig. 1. Schematics of new crown ethers 1–6.

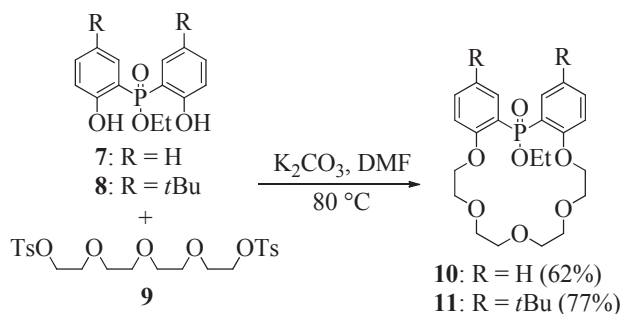
medium.

2. Results and discussion

2.1. Synthesis

Crown ethers were synthesized by macrocyclization of the reported ethyl phosphinates **7** and **8**^{5,7} and tetraethylene glycol ditosylate **9** in DMF using K₂CO₃ as a base (see Scheme 1). Synthesis of macrocycle **10** was reported earlier, but by increasing the temperature we achieved a better yield with shorter reaction time. Crown ether **11** was prepared in high yield, which is not common for a macrocyclization reaction.

The crown ethers containing an ethyl diarylphosphinate unit were nitrated using HNO₃/H₂SO₄ mixtures in CH₂Cl₂ (see Scheme 2). In the case of crown ether **10** the nitration yielded various products. In order to investigate the effect of temperature and the quantity of the reagents for the nitration, several experiments were carried out (see Table 1). The amount of H₂SO₄ was shown to have the most significant effect on the distribution of the products. Using a 2:1 ratio of HNO₃:H₂SO₄ only mono- and disubstituted crown ethers (**12** and **13**) formed, however, when H₂SO₄ was in large



Scheme 1. Macrocyclization reaction.

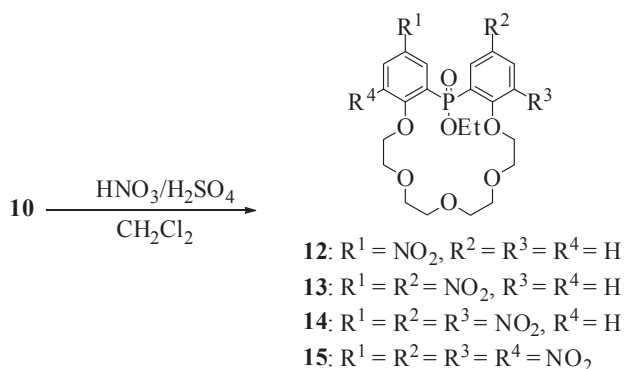
Scheme 2. Nitration of macrocycle **10**.

Table 1
Nitration of crown ether **10**.

Reagent	Temperature	Time	Product	Yield (%)
HNO ₃ /H ₂ SO ₄ 2:1	rt.	3 days	12	20
HNO ₃ /H ₂ SO ₄ 2:1	40 °C	2 days	12	13
HNO ₃ /H ₂ SO ₄ 2:1	40 °C	2 days	13	23
HNO ₃ /H ₂ SO ₄ 1:20	rt.	2 h	14	8
HNO ₃ /H ₂ SO ₄ 1:20	rt.	2 h	15	50

excess only derivatives **14** and **15** were obtained in a relatively fast reaction. As we managed to synthesize four new nitro-substituted macrocycles with an increasing number of substituents, it allowed us to investigate thoroughly the effect of nitro-substitution on the pK_a value of the diarylphosphinic acid unit in crown ethers **2–6**.

Nitration of macrocycle **11** was investigated as well (see Scheme 3 and Table 2). At the beginning the reaction did not result in the dinitro derivative **16**, which we intended to synthesize. Many reaction conditions were examined, and the reaction mixtures were analyzed using HPLC-MS. The analysis showed that the best condition for the synthesis of **16** is using a 2:1 HNO₃/H₂SO₄ mixture in boiling CH₂Cl₂ for 2 days.

Two methods were used for the hydrolysis of crown ethers containing the ethyl diarylphosphinate unit. Esters **11** and **16** were hydrolyzed with aqueous Me₄NOH in propanol (see Scheme 4). In the case of esters **11** and **16** this hydrolysis is faster and gives higher yields for acids **1** and **2** than acidic hydrolysis. Using tetramethylammonium hydroxide instead of other bases is preferred, because

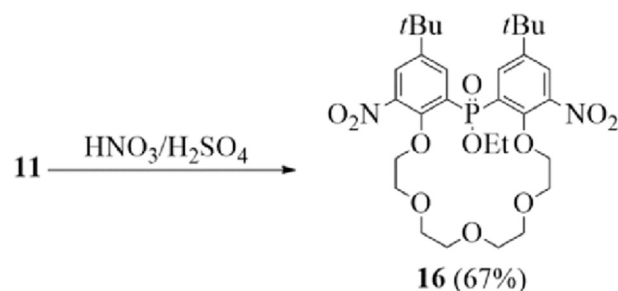
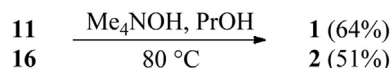
Scheme 3. Nitration of macrocycle **11**.

Table 2
Nitration of crown ether **11**.

Reagent	Solvent	Temperature	Time
HNO ₃ /H ₂ SO ₄ 2:1	CH ₂ Cl ₂	rt.	2 days
HNO ₃ /H ₂ SO ₄ 2:1	CH ₂ Cl ₂	40 °C	2 days
HNO ₃ /H ₂ SO ₄ 2:1	–	40 °C	2 days
HNO ₃	CH ₂ Cl ₂	rt.	2 days
HNO ₃	CH ₂ Cl ₂	40 °C	2 days
HNO ₃ /H ₂ SO ₄ *SO ₃ 2:1	–	rt.	3 h
HNO ₃ /H ₂ SO ₄ 2:1	CH ₂ Cl ₂	rt.	6 days

Scheme 4. Basic hydrolysis of esters **11** and **16**.

this is a fairly strong base and the absence of metal ions excludes the chance of complexation of the macrocycles.

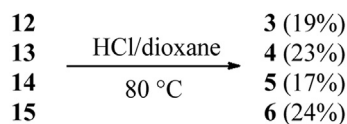
In the case of crown ethers **12–15** the nitro group on the aromatic ring in the *para* position to the ether oxygen made the aryl-alkyl ether bond less stable, and during a basic hydrolysis this bond breaks easily. Keeping this sensitivity in mind, macrocycles **12–15** were hydrolyzed in dioxane–aqueous HCl mixture, which is a slower hydrolysis, but decomposition is also much slower (see Scheme 5).

After having synthesized a series of compounds with different numbers of nitro groups and with and without *tert*-butyl substituents, we determined their pK_a values. Increasing numbers of nitro groups incorporated onto the aromatic rings were expected to lower the pK_a value of the phosphinic acid moiety, but this expectation was not fully confirmed experimentally (see below). To clarify this anomaly we synthesized the tetra-nitro-substituted phosphinic acid **17** starting from the known derivative **18**.⁸ We used the same nitration procedure as in the case of **10** to incorporate four nitro substituents (see Scheme 6).

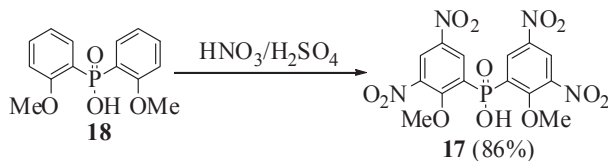
2.2. pK_a determination and related studies

pK_a Determination of six new crown ethers **1–6**, the reported **19**^{4k}, and acid derivatives **17** and **18** was accomplished with UV-pH titration, and in the case of **20**⁷ with a potentiometric method (see Table 3 and Fig. 2). In the table below the predicted and measured values are shown.

The results of the measurements revealed an anomaly. In the case of merely *para*-substituted macrocycles **19**, **1**, **3** and **4** the results were consistent with the predictions, the electron donating *tert*-butyl groups increased the pK_a values and the electron withdrawing nitro substituents decreased it. The determined values of



Scheme 5. Acidic hydrolysis of esters **12–15**.



Scheme 6. Nitration of the phosphinic acid **18**.

Table 3

Predicted and measured pK_a values of the investigated compounds.

Compound	Substituents	Predicted pK_a^a	Measured pK_a	Number of replicates	Method
19	–	2.46	3.02 ± 0.015	6	UV-pH aqueous
1	<i>p</i> -ditBu	2.68	3.15 ± 0.035	6	UV-pH aqueous
2	<i>p</i> -ditBu, <i>o</i> -diNO ₂	2.20	5.37 ± 0.087	5	UV-pH aqueous
3	<i>p</i> -NO ₂	2.15	1.54 ± 0.080	6	UV-pH MeOH
4	<i>p</i> -diNO ₂	1.90	1.48 ± 0.003	9	UV-pH MeOH
5	<i>p</i> -diNO ₂ , <i>o</i> -NO ₂	1.72	4.22 ± 0.074	16	UV-pH aqueous
6	<i>o,p</i> -tetra-NO ₂	1.58	4.23 ± 0.045	6	UV-pH aqueous
20	–	2.18	1.84 ± 0.020	3	pH-metric aqueous
18	–	2.30	2.68 ± 0.014	8	UV-pH aqueous
17	<i>o,p</i> -tetra-NO ₂	1.32	0.24 ± 0.090^b	7	UV-pH can

^a pK_a values were predicted with MarvinSketch 6.0.2 Software.

^b Extrapolated value.

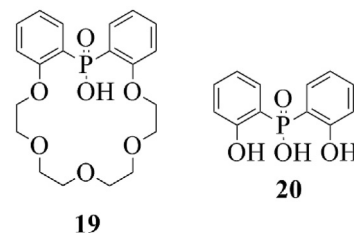


Fig. 2. Reported phosphinic acids **19** and **20** for pK_a determination. (Both acids are useful for the investigation of the effects of substituents and chemical environment on the pK_a).

crown ethers **2**, **5** and **6** contradicted the prediction and the expected behavior, because the presence of nitro substituents in the *ortho* positions to the aryl-alkyl ether bond, which are electron withdrawing groups, should have decreased the pK_a values as the predicted ones showed. Our assumption was that the nitro groups in the *ortho* positions to the aryl-alkyl ether bond caused a conformational change, which could be responsible for the reduced acidity of the macrocycles. To support this assumption parent compounds **17**, **18**⁸ and **20**⁷ were synthesized, and their pK_a values were determined. The obtained pK_a values supported our assumption, as no anomalies were observed in the measured proton-dissociation constants. In order to obtain a more sound basis for our assumption a computational study was carried out.

2.3. Modeling

As the biggest discrepancy between expected and measured pK_a values was observed in the case of **19** and **6**, these two compounds together with the highly similar phosphinic acids without the crown ether macrocycle (**18** and **17**) were investigated computationally. First a conformational search was carried out on **6** and **19**, and as expected, a large number of conformations (about 600) were predicted for both the deprotonated and neutral forms of these compounds. A conformationally diverse set of structures was subjected to quantum mechanical calculations and Fig. 3 shows the lowest energy structures predicted for **6** and **19**. In the case of **19** the overall structure of the molecule is like a “box” with an empty channel in its middle. The angle between the two phenyl rings is a bit larger than 90° and the acidic hydrogen of the phosphinic acid unit turns toward the solvent. For this reason, this conformation can be called *out*-conformation. It somewhat resembles the folding of globular proteins, the tight packing of the molecule allows favorable hydrophobic interactions between the phenyl rings and the large nonpolar crown ether macrocycle. The conjugate base form of **19** retains the overall geometry of the acidic form, although the phenyl rings are slightly more shifted compared to each other.

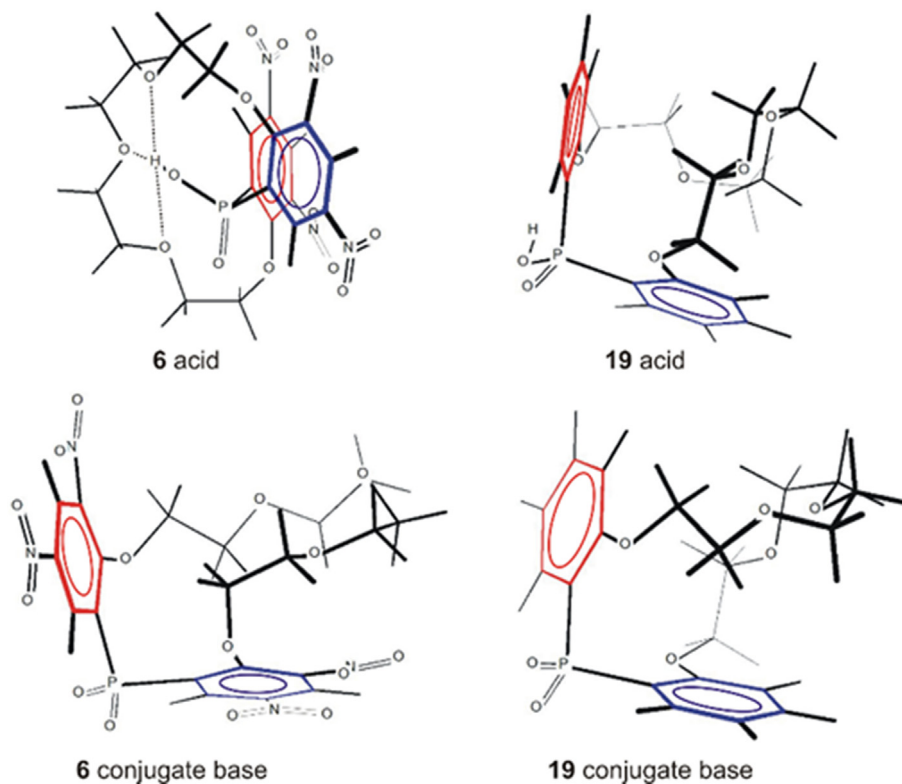
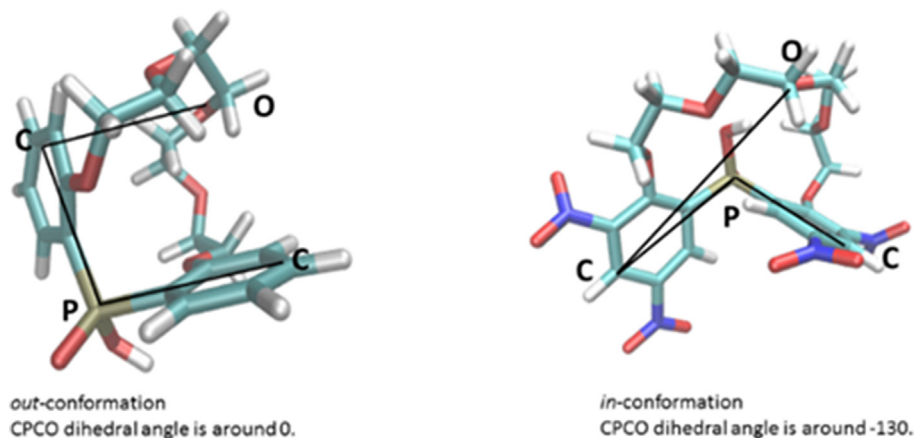


Fig. 3. Overall structure of the identified lowest energy conformers (at the M062x/6-311 + G*/PCM level) of **6** and **19** visualized by the Tapering Lines Method.⁹ Dotted lines represent the possible hydrogen bonding partners of the acidic hydrogen in **6**. The two aromatic rings are drawn in red and blue.

In contrast, the acid form of **6** exhibits a completely different geometry. The angle between the phenyl rings is increased to about 109° and the OH group of the phosphinic acid unit forms a very strong hydrogen bond with the middle crown ether oxygen (distance: 1.70 Å). Furthermore, the hydroxyl group could turn very easily toward the second or fourth crown ether oxygen to form hydrogen bonds with them. The structure suggests that the crown ether ring “embraces” the acidic proton and thereby it stabilizes this conformation. This conformation can be called *in*-conformation. The increased stability of the *in*-conformation in the case of **6** compared to **19** partly originates from (1) the large steric requirements of the nitro groups which would make the compact conformation found for **19** overcrowded for **6** (2) furthermore, due

to the large electron withdrawing effect of the four nitro groups the acidic proton is more positive in **6** than in **19** (Mullikan charges are 0.52 e and 0.49 e, respectively), which allows more favorable interactions with the crown ether oxygens. This difference is larger than the charge difference observed for **17** and **18** (0.49 and 0.50 e, respectively), where the acidic hydrogen can only interact with a single crown ether oxygen. Naturally, in the case of highly flexible compounds such as the studied crown ethers it is expected that in solution there is a fine balance among the lowest energy conformations based on their relative stabilities.

To test the diversity of conformations that **6** and **19** exhibit in solution molecular dynamics simulations were carried out for 15 ns. In both cases we monitored the changes of the conformation



Scheme 7. Definition of the CPCO dihedral angle and its respective value in the *in*- and *out*-conformations.

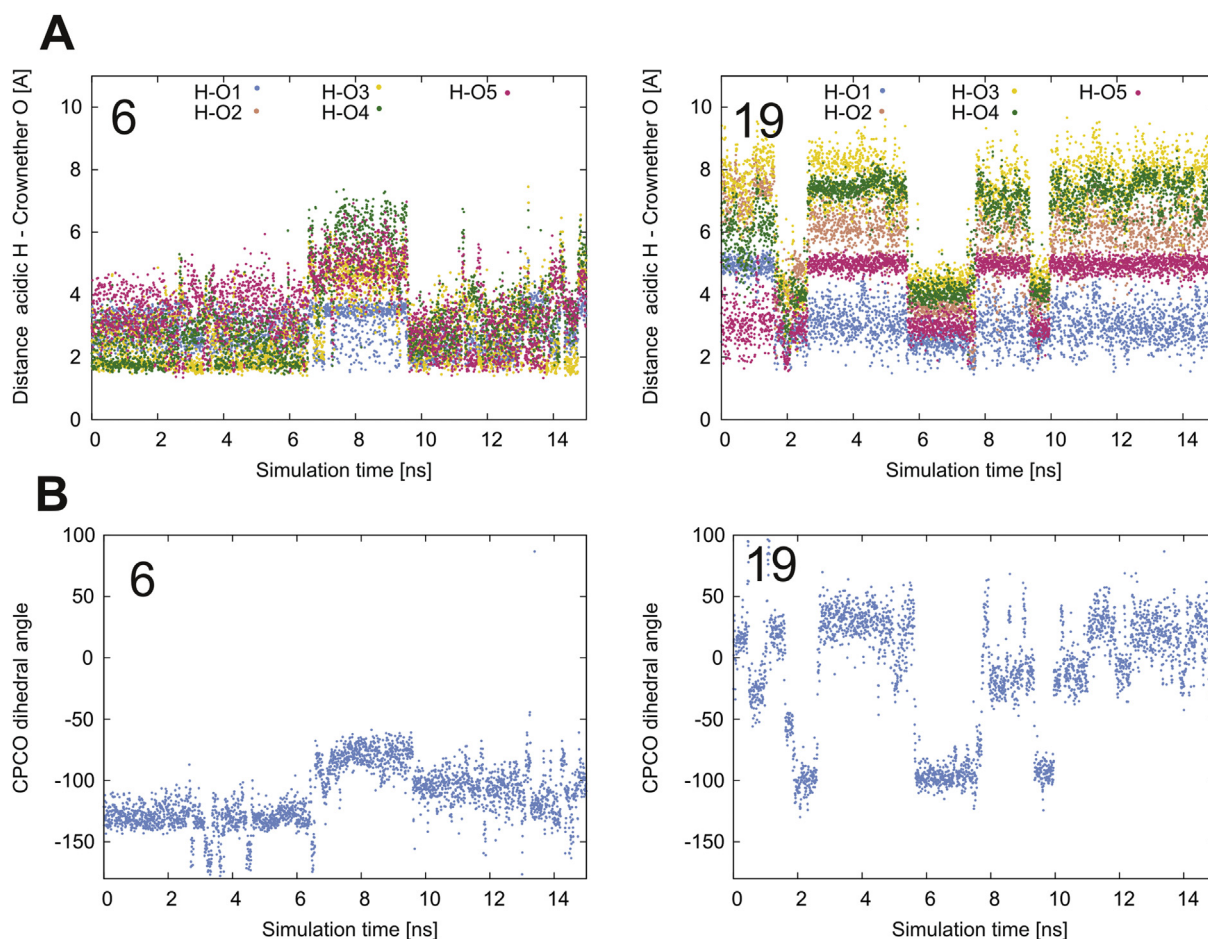


Fig. 4. Changes of (A) distances between the acidic hydrogen atom and the crown ether oxygens (B) the CPCO dihedral angle along the MD trajectories for **6** and **19**.

of the crown ether by two different properties (1) we measured the distance between the acidic hydrogen atom and the crown ether oxygens (2) by measuring the CPCO dihedral angle (see Scheme 7). It turned out that these parameters change simultaneously, thus they seem to be appropriate descriptors to characterize the overall conformation of the studied two compounds. In Fig. 4 we compared the changes of these two properties along the molecular dynamics trajectory for **6** and **19**. In the case of **19** the *in*- and *out*-conformations change frequently and the transition between them is very fast. In contrast **6** maintained its original conformation for the entire length of the simulation with a short interval where the conformation tried to change to the *out*-conformation, but it did not occur. Instead the system returned to the *in*-conformation. The results of MD simulations strongly support the suggestion that in the acidic form of **6** the conformation of the crown ether macrocycle is stabilized by strong interactions between the acidic hydrogen and the crown ether oxygens. In full accordance with this, quantum chemical calculations predicted a fine balance between the *in*- and *out*-conformations of **19**, (the *out*-conformation is predicted to be only 1.3 kcal/mol more favorable than the *in*-conformation at the M062X/6-311 + G*/PCM level of theory), while in the case of **6** the calculations predicted the *in*-conformation to be lower in energy by 7.1 kcal/mol theory. This suggests, based on the Boltzmann-distribution that the *in*-conformation will be very much in excess compared to the *out*-conformation in the case of **6**.

In Table 4 we have collected the calculated thermodynamic properties for the ionization reactions of **6** and **17–19**. **19** and **17** are characterized by similar Gibbs free energies of ionization in the gas

Table 4

Gas phase ionization energy, solvation free energy of the acid and conjugate base form of studied crown ethers containing a diarylphosphinic acid unit (in kcal/mol at the M062X/6-311 + G* level) and the pK_a value predicted using the same level of theory.

Ligand	ΔG_{gas}	$G_{\text{sol}(HA)}$	$G_{\text{sol}(A^-)}$	$\Delta G_{\text{(aq)}}$	pK _a
19	335.1	−23.1	−85.4	8.84	6.5
6	308.5	−23.9	−63.9	4.54	3.3
17	331.5	−19.7	−79.8	7.47	5.5
18	287.3	−22.6	−50.0	−4.13	−3.0

phase (335.1 and 331.5 kcal/mol, respectively), in accordance with their similar acidity determined by the experiments. Tetra-nitro-substitution of both compounds significantly reduces this value in accordance with the expectation that nitro-substitution should increase acidity. However, the decrease of the Gibbs free energies of ionization is much more significant for the acyclic compounds than for the crown ethers. This is in accordance with the conclusions drawn based on the geometries of the compounds: the acidic form of **6** is most likely greatly stabilized by the favorable interactions between the acidic hydrogen and the crown ether macrocycle, and as a consequence the ionization is less favored than in the case of the other tetra-nitro compound **18**. The solvation free energies of the acidic forms of the compounds are very similar, slightly larger values were observed for the crown ether compounds than for the acyclic ones, and nitro-substitution slightly increases the solvation free energy. In contrast, the solvation free energy of the anions shows much greater variability. The most apparent feature is that

tetra-nitro-substitution greatly reduces the solvation free energy of the anions, thus it disfavors ionization and will increase the pK_a values of the compounds. The final Gibbs free energy of the ionization reaction in solution includes the effect of all these factors, and it was used to predict the pK_a values of the compounds. Apparently the QM calculations give pK_a values in a much larger range than the observed one, which could easily originate from the error of implicit solvent models used for the calculations. The SI includes the data calculated with the B3LYP functional and two other solvation models. The observed trends are the same for all methods. Interestingly the simple pK_a prediction method of Marvin¹⁰ gives very similar trends for the pK_a value to quantum chemistry (see Table 3). In accordance with the experiment, the pK_a value of **17** is slightly lower than that of **19**, and **18** is the most acidic compound. Although the calculations do not predict **6** to be the least acidic compound, it is well reproduced that it should be much less acidic than **17**. As we see from the table that the acidity of the compounds is very sensitive to the solvation free energy of the anions, small errors in it (which are inherent to implicit solvent models) could easily account for this discrepancy. Furthermore, the assumptions used for the calculation of the entropy contribution to the Gibbs free energy (e.g. the rigid-rotor model commonly used by quantum chemical program packages) may not fully hold for largely flexible compounds such as the studied crown ethers, which also introduces some uncertainty to the obtained number. However, the obtained results are in good agreement with the experiment and they strongly support the hypothesis that upon tetra-nitro-substitution of **19** the most favorable conformation of the crown ether macrocycle underwent a significant change. In the new conformation the acidic form of **6** is significantly stabilized by hydrogen bonds to the crown ether oxygens, and this stabilization is responsible for the experimentally observed reduced acidity of **6** compared to **19**.

3. Conclusions

Six new proton-ionizable crown ethers were successfully synthesized and characterized. The pK_a determination of the new and reported compounds was performed. A wide-range study was done to reveal the anomaly of the results. As a conclusion we can declare, that the macroring oxygen atoms of these macrocycles can establish a strong hydrogen bond with the acidic proton, but this phenomenon depends on the substitution and conformation of the molecules. The effect of the hydrogen bond on the acidity of the crown ethers is great, which is demonstrated by the several orders of magnitude difference between the obtained and expected results.

4. Experimental section

General: Infrared spectra were recorded on a Bruker Alpha-T FT-IR spectrometer. Optical rotations were taken on a Perkin–Elmer 241 polarimeter that was calibrated by measuring the optical rotations of both enantiomers of menthol. ¹H NMR spectra were taken either on a Bruker DRX-500 Avance spectrometer (500 MHz, reference: TMS) or on a Bruker 300 Avance spectrometer (300 MHz, reference: TMS) and it is indicated in each individual case. ¹³C NMR spectra were taken either on a Bruker DRX-500 Avance spectrometer (125.8 MHz, reference: TMS) or on a Bruker 300 Avance spectrometer (75.5 MHz, reference: TMS) and it is indicated in each individual case. ³¹P NMR spectra were recorded on a Bruker 300 Avance spectrometer (121.5 MHz, reference: H₃PO₄). HPLC-DAD-MS/MS experiments were performed on an Agilent 1200 HPLC system (G1379B degasser, G1312B binary gradient pump, G1367C autosampler, G1316B column

thermostat and G1315C diode array detector) coupled with an Agilent 6410 triple quadrupole mass spectrometer equipped with an ESI ion source (Agilent Technologies, Waldbronn, Germany). Masshunter B.03.01 software was used for data acquisition and qualitative analyses. Elemental analyses were performed in the Microanalytical Laboratory of the Department of Organic Chemistry, Institute of Chemistry, L. Eötvös University, Budapest, Hungary. Starting materials were purchased from Sigma-Aldrich Corporation unless otherwise noted. Melting points were taken on a Boetius micro-melting point apparatus and were uncorrected. Silica gel 60 F₂₅₄ (Merck) plates were used for TLC. Silica gel 60 (70–230 mesh, Merck) were used for column chromatography. Silica gel 60 F₂₅₄ and aluminium oxide 150 F₂₅₄ (Merck) plates were used for PLC (preparative layer chromatography). Ratios of solvents for the eluents are given in volumes (mL/mL). Solvents were dried and purified according to well-established¹¹ methods. Evaporations were carried out under reduced pressure unless otherwise stated.

All pK_a determinations were carried out in aqueous medium as default, MeOH as cosolvent was used in the case of crown ethers **3**, **4** and ACN was used in the case of phosphinic acid **17** due to their poor solubility in water. The proton-dissociation constants were determined by UV-spectrophotometric titrations using D-PAS technique and potentiometric titration in the case of phosphinic acid **20** using a pH-metric method (Sirius Analytical Instruments Ltd., Forest Row, UK; attached to a Sirius T3 instrument^{12,13}) since no absorbance change related to the phosphinic acid group's deprotonation could be detected during titration. The lack of absorbance change is supposedly caused by the presence of intramolecular hydrogen bonds with the aromatic OH groups, which theory is supported by the fact that in the case of the analogue with MeO groups on the aromatic rings the proton-dissociation of the phosphinic acid group can readily be detected by absorbance changes. The pK_a values were calculated by Refinement Pro™ software. Spectrophotometry can be applied for pK_a measurement provided that the compound has a chromophore in proximity to the ionization centre, and the absorbance changes sufficiently as a function of pH. The absorbancies in the spectral region of 250–450 nm were used in the analysis. All measurements were performed in solutions of 0.15 M KCl under nitrogen atmosphere, at $t = 25.0 \pm 0.5$ °C. All pK_a values were measured in 3 or more replicates (see Table 3.).

4.1. 2,20-Di-tert-butyl-22-ethoxy-6,7,9,10,12,13,15,16-octahydro-22H-22-dibenzo[n,q]-[1,4,7,10,13,16]-pentaoxa- λ^5 -phosphacyclooctadecin-22-one (**11**)

Ethyl phosphinate **8** (3.88 g, 9.96 mmol), tetraethylene glycol ditosylate **3** (5.00 g, 9.96 mmol) and finely powdered anhydrous K₂CO₃ (38.9 g, 282 mmol) were mixed with vigorous stirring in dry DMF (470 mL) under Ar. The temperature of the reaction mixture was raised to 80 °C and kept stirring at this temperature until TLC analysis showed the total consumption of the starting materials (4 days). The solvent was removed at 40 °C, the residue was suspended in water (300 mL) and it was extracted with CH₂Cl₂ (4 × 90 mL). The combined organic phase was shaken with H₂O (60 mL), dried over MgSO₄, filtered and the solvent was removed. The crude product was purified by chromatography on silica gel using methanol–CH₂Cl₂ (1:20) as an eluent to give **11** as a yellow oil (4.21 g, 77%). The product was crystallized from hexane to give pale yellow crystals (plates). mp 95–97 °C (from hexane); R_f: 0.92 (silica gel TLC, methanol–CH₂Cl₂ 1:5); IR (neat) ν_{\max} 2954, 2901, 2866, 1600, 1488, 1460, 1361, 1263, 1128, 1090, 1080, 1033, 810, 769, 668, 588, 544 cm⁻¹; ¹H NMR (300 MHz, CD₃OD, 25 °C): $\delta = 1.34$ – 1.38 (m, 21H, CH₃), 3.18–3.39 (m, 12H, OCH₂), 4.06–4.18 (m, 6H, OCH₂),

7.09 (dd, $J = 8.6$ Hz, 6.9 Hz, 2H, ArH), 7.62 (dd, $J = 8.7$ Hz, 2.3 Hz, 2H, ArH), 7.90 (dd, $J = 14.8$ Hz, 2.5 Hz, 2H, ArH) ppm; ^{13}C NMR (75 MHz, CDCl_3 , 25 °C): $\delta = 16.6$ (d, $J = 6.8$ Hz, CH_3), 31.6 (CH_3), 34.3 (C), 60.5 (d, $J = 5.7$ Hz, OCH_2), 67.2, 69.9, 70.8, 71.3 (OCH_2), 111.7 (d, $J = 8.5$ Hz, ArC), 120.6 (d, $J = 140.8$ Hz, ArC), 129.9 (d, $J = 1.9$ Hz, ArC), 131.3 (d, $J = 6.8$ Hz, ArC), 142.8 (d, $J = 11.6$ Hz, ArC), 158.0 (d, $J = 4.2$ Hz, ArC) ppm; ^{31}P NMR (121.5 MHz, CDCl_3 , 25 °C): $\delta = 28.2$ ppm; MS: 549.3 ($\text{M}+\text{H}$) $^+$; Anal. Calcd for $\text{C}_{30}\text{H}_{45}\text{O}_7\text{P}$: C, 65.67; H, 8.27. Found: C, 65.52; H, 8.28.

General procedure for nitration: The crown ether was solved in CH_2Cl_2 and mixture of *cc.* H_2SO_4 and *cc.* HNO_3 was added to it at 0 °C. After the addition the temperature was raised to room temperature, and the mixture was stirred until TLC analysis showed the total consumption of the starting crown ether. CH_2Cl_2 (6 vol for the starting crown ether) and H_2O (8 vol for the starting crown ether) were added to the mixture, and the phases were separated. The aqueous phase was extracted with CH_2Cl_2 (4 vol for the starting crown ether, 3x). The combined organic phase was dried over MgSO_4 , and the solvent was removed. The crown ethers were purified by chromatography on silica gel using methanol– CH_2Cl_2 as an eluent.

4.2. 22-Ethoxy-2-nitro-6,7,9,10,12,13,15,16-octahydro-22H-22-dibenzo[n,q]-[1,4,7,10,13,16]pentaaxa- λ^5 -phosphacyclooctadecin-22-one (**12**)

Macrocycle **10** (1.50 g, 3.44 mmol), CH_2Cl_2 (15 mL), $\text{HNO}_3/\text{H}_2\text{SO}_4$ (0.95 mL, 2:1), room temperature. Reaction time: 1 day, yield: 0.32 g (20%), yellow powder. mp 101–104 °C (from methanol); R_f : 0.54 (silica gel TLC, methanol– CH_2Cl_2 1:10); IR (KBr) ν_{max} 3105, 3071, 3029, 2985, 2900, 1605, 1592, 1580, 1515, 1475, 1444, 1342, 1290, 1259, 1233, 1211, 1144, 1035, 950, 941, 838, 794, 754, 563, 522 cm^{-1} ; ^1H NMR (500 MHz, CDCl_3 , 25 °C): $\delta = 1.30$ (t, $J = 7.0$ Hz, 3H, CH_3), 3.06–3.33 (m, 12H, OCH_2), 3.98–4.15 (m, 4H, OCH_2), 4.18–4.28 (m, 2H, OCH_2), 6.92 (dd, $J = 8.0$ Hz, 6.7 Hz, 1H, ArH), 7.04 (td, $J = 7.4$ Hz, 2.5 Hz, 1H, ArH), 7.08 (dd, $J = 9.2$ Hz, 5.9 Hz, 1H, ArH), 7.45 (td, $J = 8.2$ Hz, 1.3 Hz, 1H, ArH), 8.00 (dd, $J = 13.8$ Hz, 7.5 Hz, 1H, ArH), 8.25 (dd, $J = 9.2$ Hz, 2.8 Hz, 1H, ArH), 8.77 (dd, $J = 14.1$ Hz, 2.4 Hz, 1H, ArH) ppm; ^{13}C NMR (125 MHz, CDCl_3 , 25 °C) $\delta = 16.5$ (d, $J = 6.5$ Hz, CH_3), 61.0 (d, $J = 5.7$ Hz, OCH_2), 67.3, 67.9, 69.9, 70.2, 70.6, 71.0, 71.2, 71.5, (OCH_2), 111.9 (d, $J = 7.9$ Hz, ArC), 112.7 (d, $J = 7.9$ Hz, ArC), 119.3 (d, $J = 142.9$ Hz, ArC), 120.4 (d, $J = 12.8$ Hz, ArC), 122.8 (d, $J = 142.7$ Hz, ArC), 128.5 (d, $J = 1.4$ Hz, ArC), 130.4 (d, $J = 7.3$ Hz, ArC), 134.0 (d, $J = 1.6$ Hz, ArC), 135.0 (d, $J = 6.1$ Hz, ArC), 140.9 (d, $J = 14.5$ Hz, ArC), 160.3 (d, $J = 4.1$ Hz, ArC), 165.2 (d, $J = 4.5$ Hz, ArC) ppm; ^{31}P NMR (121.5 MHz, CDCl_3 , 25 °C): $\delta = 23.6$; MS: 482.1 ($\text{M}+\text{H}$) $^+$, 504.2 ($\text{M}+\text{Na}$) $^+$; Anal. Calcd for $\text{C}_{22}\text{H}_{28}\text{NO}_9\text{P}$: C, 54.89; H, 5.86; N, 2.91. Found: C, 54.68; H, 5.70; N, 3.07.

4.3. 22-Ethoxy-2,20-dinitro-6,7,9,10,12,13,15,16-octahydro-22H-22-dibenzo[n,q]-[1,4,7,10,13,16]pentaaxa- λ^5 -phosphacyclooctadecin-22-one (**13**)

Macrocycle **10** (1.71 g, 3.92 mmol), CH_2Cl_2 (15 mL), $\text{HNO}_3/\text{H}_2\text{SO}_4$ (1.08 mL, 2:1), 40 °C. Reaction time: 1 day, yield: 0.48 g (23%), yellow powder. mp 188–192 °C (from methanol); R_f : 0.66 (silica gel TLC, methanol– CH_2Cl_2 1:10); IR (KBr) ν_{max} 3068, 2969, 2913, 2876, 1600, 1583, 1514, 1476, 1340, 1288, 1266, 1215, 1153, 1033, 969, 929, 891, 833, 790, 753, 560 cm^{-1} ; ^1H NMR (500 MHz, CDCl_3 , 25 °C): $\delta = 1.34$ (t, $J = 7.0$ Hz, 3H, CH_3), 3.13–3.24 (m, 12H, OCH_2), 4.10–4.27 (m, 6H, OCH_2), 7.08 (dd, $J = 9.1$ Hz, 6.2 Hz, 2H, ArH), 8.31 (dd, $J = 9.2$ Hz, 2.7 Hz, 2H, ArH), 8.85 (dd, $J = 14.3$ Hz, 2.6 Hz, 2H, ArH) ppm; ^{13}C NMR (125 MHz, CDCl_3 , 25 °C): $\delta = 16.5$ (d, $J = 6.2$ Hz, CH_3), 61.6 (d, $J = 5.6$ Hz, OCH_2), 68.1, 70.0, 70.7, 71.3 (OCH_2), 112.5 (d, $J = 7.9$ Hz, ArC), 121.2 (d, $J = 143.6$ Hz, ArC), 129.2 (d, $J = 1.6$ Hz, ArC),

130.8 (d, $J = 7.3$ Hz, ArC), 141.1 (d, $J = 14.8$ Hz, ArC), 165.1 (d, $J = 4.5$ Hz, ArC) ppm; ^{31}P NMR (121.5 MHz, CDCl_3 , 25 °C): $\delta = 20.1$ ppm; MS: 527.1 ($\text{M}+\text{H}$) $^+$, 549.1 ($\text{M}+\text{Na}$) $^+$; Anal. Calcd for $\text{C}_{22}\text{H}_{27}\text{N}_2\text{O}_{11}\text{P}$: C, 50.19; H, 5.17; N, 5.32. Found: C, 49.93; H, 5.04; N, 5.02.

4.4. 22-Ethoxy-2,4,20-trinitro-6,7,9,10,12,13,15,16-octahydro-22H-22-dibenzo[n,q]-[1,4,7,10,13,16]pentaaxa- λ^5 -phosphacyclooctadecin-22-one (**14**)

Macrocycle **10** (2.48 g, 5.69 mmol), CH_2Cl_2 (20 mL), HNO_3 (0.6 mL), H_2SO_4 (10.0 mL), room temperature. Reaction time: 2 h, yield: 0.26 g (8%), dark yellow powder. mp 159–161 °C (from methanol); R_f : 0.75 (silica gel TLC, methanol– CH_2Cl_2 1:10); IR (KBr) ν_{max} 3107, 3079, 2905, 1604, 1525, 1475, 1451, 149, 1343, 1280, 1244, 1147, 1131, 1093, 1065, 1028, 937, 753, 651, 563 cm^{-1} ; ^1H NMR (300 MHz, CD_3OD , 25 °C): $\delta = 1.43$ (t, $J = 7.0$ Hz, 3H, CH_3), 2.72–2.76 (m, 2H, OCH_2), 2.99–3.03 (m, 2H, OCH_2), 3.16–3.21 (m, 4H, OCH_2), 3.33–3.35 (m, 2H, OCH_2), 3.65–3.68 (m, 2H, OCH_2), 4.16–4.25 (m, 6H, OCH_2), 7.33 (dd, $J = 9.2$ Hz, 6.6 Hz 1H, ArH), 8.53 (dd, $J = 9.2$ Hz, 2.8 Hz 1H, ArH), 8.82–8.88 (m, 2H, ArH), 8.99 (dd, $J = 13.9$ Hz, 2.8 Hz 1H, ArH) ppm; ^{13}C NMR (75 MHz, CDCl_3 , 25 °C): $\delta = 16.6$ (d, $J = 6.1$ Hz, CH_3), 62.5 (d, $J = 5.8$ Hz, OCH_2), 68.7, 69.3, 69.8, 70.1, 70.2, 70.6, 71.2, 72.9 (OCH_2), 112.1 (d, $J = 8.3$ Hz, ArC), 120.5 (d, $J = 146.3$ Hz, ArC), 125.1 (d, $J = 1.7$ Hz, ArC), 128.9 (d, $J = 139.0$ Hz, ArC), 130.3 (d, $J = 1.4$ Hz, ArC), 130.5 (d, $J = 6.8$ Hz, ArC) 135.1 (d, $J = 7.9$ Hz, ArC), 141.3 (d, $J = 14.9$ Hz, ArC), 141.5 (d, $J = 11.1$ Hz, ArC), 141.7 (d, $J = 6.2$ Hz, ArC), 158.5 (d, $J = 5.3$ Hz, ArC), 165.1 (d, $J = 4.9$ Hz, ArC) ppm; ^{31}P NMR (121.5 MHz, CDCl_3 , 25 °C): $\delta = 18.3$ ppm; MS: 572.1 ($\text{M}+\text{H}$) $^+$, 594.1 ($\text{M}+\text{Na}$) $^+$; Anal. Calcd for $\text{C}_{22}\text{H}_{26}\text{N}_3\text{O}_{13}\text{P}$: C, 46.24; H, 4.59; N, 7.35. Found: C, 46.22; H, 4.66; N, 7.42.

4.5. 22-Ethoxy-2,4,18,20-tetranitro-6,7,9,10,12,13,15,16-octahydro-22H-22-dibenzo[n,q]-[1,4,7,10,13,16]pentaaxa- λ^5 -phosphacyclooctadecin-22-one (**15**)

Macrocycle **10** (2.48 g, 5.69 mmol), CH_2Cl_2 (20 mL), HNO_3 (0.6 mL), H_2SO_4 (10.0 mL), room temperature. Reaction time: 2 h, yield: 1.75 g (50%), dark yellow powder. mp 159–161 °C (from methanol); R_f : 0.79 (silica gel TLC, methanol– CH_2Cl_2 1:10); IR (KBr) ν_{max} 3101, 3080, 3029, 2906, 2868, 1601, 1540, 1471, 1442, 1408, 1343, 1243, 1132, 1108, 1091, 1022, 976, 940, 885, 785, 743, 684, 566 cm^{-1} ; ^1H NMR (500 MHz, CDCl_3 , 25 °C): $\delta = 1.44$ (t, $J = 7.1$ Hz, 3H, CH_3), 3.18–3.24 (m, 8H, OCH_2), 3.26–3.30 (m, 2H, OCH_2), 3.38–3.42 (m, 2H, OCH_2), 3.46 (s, 3H, complexed MeOH), 4.09–4.13 (m, 2H, OCH_2), 4.21–4.27 (m, 2H, OCH_2), 4.30–4.34 (m, 2H, OCH_2), 8.78 (d, $J = 2.8$ Hz, 2H, ArH), 9.04 (dd, $J = 13.9$ Hz, 2.8 Hz 2H, ArH) ppm; ^{13}C NMR (125 MHz, CDCl_3 , 25 °C): $\delta = 16.6$ (d, $J = 5.8$ Hz, CH_3), 63.1 (d, $J = 5.8$ Hz, OCH_2), 69.2, 69.5, 70.0, 73.6 (OCH_2), 125.7 (d, $J = 1.8$ Hz, ArC), 128.7 (d, $J = 144.7$ Hz, ArC), 133.5 (d, $J = 7.4$ Hz, ArC), 141.3 (d, $J = 11.0$ Hz, ArC), 141.6 (d, $J = 16.1$ Hz, ArC), 158.3 (d, $J = 5.6$ Hz, ArC) ppm; ^{31}P NMR (121.5 MHz, CDCl_3 , 25 °C): $\delta = 17.0$ ppm; MS: 634.1 ($\text{M}+\text{NH}_4$) $^+$; Anal. Calcd for $\text{C}_{22}\text{H}_{25}\text{N}_4\text{O}_{15}\text{P}$ ·MeOH: C, 42.60; H, 4.51; N, 8.64. Found: C, 42.33; H, 4.34; N, 8.39.

4.6. 2,20-Di-tert-butyl-22-ethoxy-4,18-dinitro-6,7,9,10,12,13,15,16-octahydro-22H-22-dibenzo[n,q]-[1,4,7,10,13,16]pentaaxa- λ^5 -phosphacyclooctadecin-22-one (**16**)

Macrocycle **11** (0.92 g, 1.68 mmol), CH_2Cl_2 (10 mL), $\text{HNO}_3/\text{H}_2\text{SO}_4$ (1.0 mL, 2:1), 40 °C. Reaction time: 6 days, yield: 0.72 g (67%), yellow oil. R_f : 0.27 (silica gel TLC, methanol–toluene 1:10); IR (neat) ν_{max} 2962, 2905, 2870, 1605, 1560, 1530, 1477, 1444, 1364, 1350,

1236, 1109, 1023, 950, 896, 876, 864, 800, 729, 646, 617, 558 cm⁻¹; ¹H NMR (500 MHz, CDCl₃, 25 °C): δ = 1.33 (s, 18H, CH₃), 1.40 (t, *J* = 7.0 Hz, 3H, CH₃), 3.32–3.43 (m, 8H, OCH₂), 3.51–3.60 (m, 4H, OCH₂), 4.02–4.06 (m, 2H, OCH₂), 4.18–4.24 (m, 2H, OCH₂), 4.28–4.32 (m, 2H, OCH₂), 7.96 (d, *J* = 2.4 Hz, 2H, ArH), 8.00 (dd, *J* = 14.4 Hz, 2.3 Hz, 2H, ArH) ppm; ¹³C NMR (125 MHz, CDCl₃, 25 °C): δ = 16.6 (d, *J* = 6.2 Hz, CH₃), 31.2 (CH₃), 35.0 (C), 62.1 (d, *J* = 6.1 Hz, OCH₂), 69.7, 70.4, 70.8, 74.7 (OCH₂), 126.5 (d, *J* = 1.5 Hz, ArC), 128.6 (d, *J* = 141.0 Hz, ArC), 135.1 (d, *J* = 7.8 Hz, ArC), 143.8 (d, *J* = 12.1 Hz, ArC), 147.5 (d, *J* = 12.6 Hz, ArC), 153.0 (d, *J* = 5.2 Hz, ArC) ppm; ³¹P NMR (121.5 MHz, CDCl₃, 25 °C): δ = 24.7 ppm; MS: 639.3 (M+H)⁺, 661.3 (M+23)⁺; Anal. Calcd for C₃₀H₄₃N₂O₁₁P: C, 56.42; H, 6.79; N, 4.39. Found: C, 56.27; H, 6.86; N, 4.32.

4.7. 2,20-Di-*tert*-butyl-22-hydroxy-6,7,9,10,12,13,15,16-octahydro-22H-22-dibenzo[*n,q*][1,4,7,10,13,16]-pentaoxa-λ⁵-phosphacyclooctadecin-22-one (**1**)

To a vigorously stirred solution of ethyl phosphinate **11** (0.28 g, 0.51 mmol) in propanol (5 mL) 25% aqueous Me₄NOH (2 mL) was added at rt. The reaction mixture was boiled with stirring until TLC analysis showed the total consumption of the starting **11** (6 days). Propanol was removed at 40 °C, H₂O (20 mL) and CH₂Cl₂ (10 mL) were added and the pH of the mixture was adjusted to 1 with 10% aqueous HCl (4 mL). The phases were separated and the aqueous phase was extracted with CH₂Cl₂ (3 × 10 mL). The combined organic phase was dried over MgSO₄, filtered and the solvent was removed. The residue (0.30 g) was purified by triturating with ethanol (3 mL) to give **1** (0.17 g, 64%) as white crystals (plates). mp 245–247 °C (from ethanol); R_f: 0.11 (silica gel TLC, methanol–CH₂Cl₂ 1:10); IR (KBr) ν_{max} 3432 (br), 3081, 3036, 2959, 2903, 2868, 1601, 1574, 1491, 1395, 1362, 1296, 1265, 1233, 1164, 1130, 1090, 949, 810, 740, 668, 585, 547 cm⁻¹; ¹H NMR (500 MHz, CDCl₃, 25 °C): δ = 1.20 (s, 18H, CH₃), 3.47–3.54 (m, 12H, OCH₂), 4.08–4.10 (m, 4H, OCH₂), 6.81 (dd, *J* = 8.6 Hz, 6.1 Hz, 2H, ArH), 7.40 (dd, *J* = 8.6 Hz, 2.4 Hz, 2H, ArH), 7.68 (dd, *J* = 15.8 Hz, 2.5 Hz, 2H, ArH), 8.61 (broad s, 1H, P-OH) ppm; ¹³C NMR (75 MHz, CDCl₃, 25 °C): δ = 31.4 (CH₃), 34.3 (C), 68.2, 69.5, 70.5, 71.4 (OCH₂), 111.6 (d, *J* = 7.9 Hz, ArC), 121.2 (d, *J* = 139.4 Hz, ArC), 129.9 (d, *J* = 1.8 Hz, ArC), 131.0 (d, *J* = 9.6 Hz, ArC), 143.2 (d, *J* = 12.4 Hz, ArC), 157.8 (d, *J* = 2.5 Hz, ArC) ppm; ³¹P NMR (121.5 MHz, CDCl₃, 25 °C): δ = 29.7 ppm; HRMS Calcd for C₂₈H₄₂O₇P: 521.2663. Found: 526.2158 (M+H)⁺.

4.8. 2,20-Di-*tert*-butyl-22-hydroxy-4,18-dinitro-6,7,9,10,12,13,15,16-octahydro-22H-22-dibenzo[*n,q*][1,4,7,10,13,16]-pentaoxa-λ⁵-phosphacyclooctadecin-22-one (**2**)

Macrocycle **2** was prepared from **16** (0.72 g, 1.13 mmol) in the same way as described above for **1**. The reaction temperature was 50 °C, the reaction was completed in 6 h. The crude product was purified by chromatography on silica gel using methanol–CH₂Cl₂ 1:30 as an eluent to give **2** (0.35 g, 51%) as a yellow powder. mp 304–307 °C (from methanol); R_f: 0.31 (silica gel TLC, methanol–CH₂Cl₂ 1:10); IR (KBr) ν_{max} 3418 (br), 3080, 2964, 2909, 2875, 1605, 1557, 1530, 1478, 1453, 1359, 1272, 1250, 1237, 1207, 1156, 1129, 1111, 1061, 944, 895, 868, 735, 573, 552 cm⁻¹; ¹H NMR (300 MHz, CD₃OD, 25 °C): δ = 1.28 (s, 18H, CH₃), 3.69–3.75 (m, 12H, OCH₂), 3.97 (broad s, 4H, OCH₂), 7.90–7.94 (m, 4H, ArH) ppm; ¹³C NMR (75 MHz, CD₃OD, 25 °C): δ = 31.3 (CH₃), 35.7 (C), 69.2, 70.0, 70.3, 76.1 (OCH₂), 125.3 (d, *J* = 2.0 Hz, ArC), 136.5 (d, *J* = 8.2 Hz, ArC), 136.5 (d, *J* = 129.3 Hz, ArC), 145.5 (d, *J* = 10.7 Hz, ArC), 149.3 (d, *J* = 11.5 Hz, ArC), 151.4 (d, *J* = 4.0 Hz, ArC) ppm; ³¹P NMR (121.5 MHz, CD₃OD, 25 °C): δ = 10.2 ppm; HRMS Calcd for C₂₈H₄₀N₂O₁₁P: 611.2364. Found: 611.2369 (M+H)⁺.

General procedure for acidic hydrolysis: To ethyl phosphinate crown ether dioxane and 10% aqueous HCl were added. The mixture was stirred vigorously at 80 °C until TLC analysis showed the total consumption of the starting crown ether. Dioxane was removed at 40 °C, after which H₂O (20 vol for the starting crown ether) and CH₂Cl₂ (40 vol for the starting crown ether) were added. The phases were separated and the aqueous phase was extracted with CH₂Cl₂ (40 vol for the starting crown ether, 3 ×). The combined organic phase was dried over MgSO₄, filtered and the solvent was removed. The residue was purified by PLC using methanol–CH₂Cl₂ as eluent or triturated with ethanol.

4.9. 22-Hydroxy-2-nitro-6,7,9,10,12,13,15,16-octahydro-22H-22-dibenzo[*n,q*][1,4,7,10,13,16]-pentaoxa-λ⁵-phosphacyclooctadecin-22-one (**3**)

Macrocycle **12** (0.23 g, 0.48 mmol), dioxane (15 mL), aqueous HCl (15 mL). The residue was purified by PLC using methanol–CH₂Cl₂ (1:8) as an eluent. Reaction time: 6 days, yield: 0.041 g, (19%), yellow crystals (plates). mp 107–111 °C (from methanol); R_f: 0.55 (silica gel TLC, methanol–CH₂Cl₂ 1:5); IR (KBr) ν_{max} 3424 (br), 1604, 1590, 1580, 1510, 1478, 1441, 1340, 1276, 1143, 1096, 1072, 1034, 972, 893, 756, 565 cm⁻¹; ¹H NMR (300 MHz, CD₃OD, 25 °C): δ = 3.50–3.53 (m, 2H, OCH₂), 3.65–3.73 (m, 12H, OCH₂), 3.76 (s, 3H, complexed MeOH), 3.94–3.97 (m, 2H, OCH₂), 6.88 (dd, *J* = 8.0 Hz, 5.7 Hz, 1H, ArH), 7.03 (dd, *J* = 9.0 Hz, 5.2 Hz, 2H, ArH), 7.35–7.40 (m, 1H, ArH), 7.93 (ddd, *J* = 13.5 Hz, 7.5 Hz, 1.5 Hz, 1H, ArH), 8.29 (dd, *J* = 9.1 Hz, 2.9 Hz, 1H, ArH), 8.88 (dd, *J* = 13.4 Hz, 2.9 Hz, 1H, ArH) ppm; ¹³C NMR (75 MHz, CD₃OD, 25 °C): δ = 56.5, 61.7, 68.0, 70.6, 70.6, 70.9, 71.2, 73.4 (OCH₂), 112.2 (d, *J* = 6.8 Hz, ArC), 112.9 (d, *J* = 7.2 Hz, ArC), 121.5 (d, *J* = 12.0 Hz, ArC), 127.8 (d, *J* = 138.3 Hz, ArC), 128.9 (d, *J* = 1.4 Hz, ArC), 130.5 (d, *J* = 130.5 Hz, ArC), 130.9 (d, *J* = 7.3 Hz, ArC), 133.2 (d, *J* = 1.5 Hz, ArC), 135.2 (d, *J* = 6.4 Hz, ArC), 142.1 (d, *J* = 13.3 Hz, ArC), 160.8 (d, *J* = 3.6 Hz, ArC), 167.1 (d, *J* = 4.0 Hz, ArC) ppm; ³¹P NMR (121.5 MHz, CD₃OD, 25 °C): δ = 10.4 ppm; HRMS Calcd for C₂₀H₂₅N₂O₉P·MeOH: 486.1524. Found: 486.1522 (M·MeOH+H)⁺.

4.10. 22-Hydroxy-2,20-dinitro-6,7,9,10,12,13,15,16-octahydro-22H-22-dibenzo[*n,q*]-[1,4,7,10,13,16]pentaoxa-λ⁵-phosphacyclooctadecin-22-one (**4**)

Macrocycle **13** (0.20 g, 0.38 mmol), dioxane (15 mL), aqueous HCl (15 mL). The crude product (0.3 g) was triturated with ethanol (3 mL). Reaction time: 6 days, yield: 0.044 g, (23%), pale yellow crystals (plates). mp 315 °C (from ethanol, decomposition); R_f: 0.34 (silica gel TLC, methanol–CH₂Cl₂ 1:10); IR (KBr) ν_{max} 3424 (br), 1604, 1581, 1480, 1455, 1344, 1278, 1178, 1083, 952, 752, 652, 594, 566 cm⁻¹; ¹H NMR (300 MHz, DMSO-D₆, 25 °C): δ = 3.08–3.16 (m, 12H, OCH₂), 4.22–4.25 (m, 4H, OCH₂), 7.32 (dd, *J* = 8.9 Hz, 6.1 Hz, 2H, ArH), 8.36 (dd, *J* = 9.0 Hz, 2.3 Hz, 2H, ArH), 8.64 (dd, *J* = 14.4 Hz, 2.4 Hz, 2H, ArH) ppm; ¹³C NMR (75 MHz, DMSO-D₆, 25 °C): δ = 67.6, 69.3, 70.2, 70.4 (OCH₂), 113.3 (d, *J* = 7.2 Hz, ArC), 123.5 (d, *J* = 140.1 Hz, ArC), 128.7 (d, *J* = 1.3 Hz, ArC), 129.2 (d, *J* = 7.8 Hz, ArC), 140.1 (d, *J* = 14.5 Hz, ArC), 164.8 (d, *J* = 4.2 Hz, ArC) ppm; ³¹P NMR (121.5 MHz, DMSO-D₆, 25 °C): δ = 13.8 ppm; HRMS: Calcd for C₂₀H₂₄N₂O₁₁P: 499.1112. Found: 499.1112 (M+H)⁺.

4.11. 22-Hydroxy-2,4,20-trinitro-6,7,9,10,12,13,15,16-octahydro-22H-22-dibenzo[*n,q*]-[1,4,7,10,13,16]pentaoxa-λ⁵-phosphacyclooctadecin-22-one (**5**)

Macrocycle **14** (0.26 g, 0.46 mmol), dioxane (15 mL), aqueous HCl (15 mL). The crude product was purified by PLC using methanol–CH₂Cl₂ (1:10) as an eluent. Reaction time: 6 days, yield:

0.042 g, (17%), yellow crystals (plates). mp 319–321 °C (from methanol); R_f : 0.48 (silica gel TLC, methanol–CH₂Cl₂ 1:5); IR (KBr): ν_{\max} 3433 (br), 3091, 1603, 1586, 1535, 1522, 1509, 1472, 1453, 1344, 1271, 1250, 1127, 1094, 1054, 949, 935, 890, 756, 652, 551 cm⁻¹; ¹H NMR (500 MHz, CD₃OD, 25 °C): δ = 3.40–3.62 (m, 12H), 4.15–4.17 (m, 2H), 4.38 (m, 2H), 7.17 (dd, J = 9.2 Hz, 5.3 Hz, 1H), 8.34 (dd, J = 9.1 Hz, 2.9 Hz, 1H), 8.70 (d, J = 2.8 Hz, 1H), 8.76 (dd, J = 13.4 Hz, 2.6 Hz, 1H), 8.92 (dd, J = 13.6 Hz, 2.9 Hz, 1H) ppm; ¹³C NMR (125.7 MHz, CD₃OD, 25 °C): δ = 69.5, 70.0, 70.2, 70.5, 70.6, 70.7, 71.1, 76.6 (OCH₂), 113.5 (d, J = 7.1 Hz, ArC), 123.6 (d, J = 2.1 Hz, ArC), 129.3 (d, J = 135.7 Hz, ArC), 129.5 (d, J = 1.7 Hz, ArC), 129.8 (d, J = 7.1 Hz, ArC), 134.3 (d, J = 9.1 Hz, ArC), 138.8 (d, J = 125.4 Hz, ArC), 142.5 (d, J = 13.7 Hz, ArC), 143.7 (d, J = 13.9 Hz, ArC), 145.2 (d, J = 10.5 Hz, ArC), 158.7 (d, J = 4.3 Hz, ArC), 165.6 (d, J = 3.4 Hz, ArC) ppm; ³¹P NMR (161.8 MHz, CD₃OD, 25 °C): δ = 6.7 ppm; HRMS Calcd for C₂₀H₂₁N₃O₁₃P: 542.0818. Found: 542.0820 (M–H)⁻.

4.12. 22-Hydroxy-2,4,18,20-tetranitro-6,7,9,10,12,13,15,16-octahydro-22H-22-dibenzof[n,q]-[1,4,7,10,13,16]pentaoxa- λ^5 -phosphacyclooctadecin-22-one (**6**)

Macrocycle **15** (0.20 g, 0.32 mmol), dioxane (15 mL), aqueous HCl (15 mL). The crude product was triturated with methanol. Reaction time: 5 days, yield: 0.046 g, (24%), darkyellow crystals (plates). mp 253–255 °C (from methanol); R_f : 0.16 (silica gel TLC, methanol–CH₂Cl₂ 1:15); IR (KBr) ν_{\max} 3417 (br), 3091, 2912, 1604, 1589, 1537, 1444, 1402, 1346, 1251, 1127, 1091, 1066, 937, 874, 744, 685, 560 cm⁻¹; ¹H NMR (800 MHz, CD₃OD, 25 °C): δ = 3.487–3.492 (m, 8H, OCH₂), 3.565–3.574 (m, 4H, OCH₂), 4.18 (br s, 4H, OCH₂), 8.79 (d, J = 2.8 Hz, 2H, ArH), 8.88 (dd, J = 13.2 Hz, 2.8 Hz, 2H, ArH) ppm; ¹³C NMR (201 MHz, CD₃OD, 25 °C): δ = 70.0, 70.2, 70.8, 75.8 (OCH₂), 124.7 (d, J = 1.3 Hz, ArC), 133.2 (d, J = 8.4 Hz, ArC), 138.1 (d, J = 130.3 Hz, ArC), 143.7 (d, J = 14.5 Hz, ArC), 144.5 (d, J = 9.5 Hz, ArC), 158.5 (d, J = 4.1 Hz, ArC) ppm; ³¹P NMR (121.5 MHz, CD₃OD, 25 °C): δ = 5.4 ppm; HRMS Calcd for C₂₀H₂₂N₄O₁₅P: 589.0814. Found: 589.0813 (M+H)⁺.

4.13. Bis(2-methoxy-3,5-dinitrophenyl)phosphinic acid (**17**)

To bisphosphinic acid **18** (0.10 g, 0.36 mmol) cc. HNO₃ (0.07 mL, 1.62 mmol) and cc. H₂SO₄ (1.10 mL, 20 mmol) were added. The resulting mixture was stirred at rt for 30 min, then at 60 °C for additional 30 min. The reaction was monitored by TLC, the whole amount of starting material was transformed. The mixture was cooled to rt, then water (1 mL) was added to it, the resulting yellow precipitation was filtered and washed with water to give **17** (0.14 g, 86%) as a pale yellow powder. mp 206–209 °C (from water); R_f : 0.40 (silica gel TLC, methanol–EtOAc 1:4); IR (KBr): ν_{\max} 3433 (br), 3089, 2964, 2869, 1599, 1536, 1475, 1417, 1345, 1265, 1203, 1086, 984, 933, 884, 746, 679, 555, 460 cm⁻¹; ¹H NMR (500 MHz, DMSO-D₆, 25 °C): δ = 3.67 (s, 6H, CH₃), 8.86 (dd, J = 13.3 Hz, 2.7 Hz, 2H, ArH), 8.93 (d, J = 2.8 Hz, 2H, ArH) ppm; ¹³C NMR (125 MHz, DMSO-D₆, 25 °C): δ = 63.3 (s, CH₃), 125.1 (d, J = 1.7 Hz, ArC), 131.7 (d, J = 7.7 Hz, ArC), 133.4 (d, J = 137.8 Hz, ArC), 142.2 (d, J = 26.6 Hz, ArC), 142.3 (d, J = 0.5 Hz, ArC), 158.2 (d, J = 5.3 Hz, ArC) ppm; ³¹P NMR (121.5 MHz, DMSO-D₆, 25 °C): δ = 7.2 ppm; HRMS Calcd for C₁₄H₁₀N₄O₁₂P: 457.0038. Found: 457.0037 (M–H)⁻.

5. Computational details

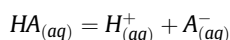
First an exhaustive conformational search was carried out with a mixed torsional/Low-mode sampling using MacroModel¹⁴ of the Schrödinger program package for the neutral and deprotonated forms of **6** and **19** in water and various structurally significantly

different conformations were chosen for quantum mechanical calculations.

(1) Quantum chemical calculations

Calculations were carried out with the Gaussian 09 program package¹⁵ using the dispersion-corrected M062X functional of the Minnesota series.¹⁶ The geometries were fully optimized using the 6-31G(d) basis set and the PCM solvent model using water as the solvent to account for the interaction of the molecule with the solvent. Second derivative calculations were carried out at the same level of theory in the PCM solvent in order to ensure that the structures were minima on the potential energy surface and to obtain the thermal correction to the Gibbs Free energy of the systems at 298.15 K and 1 atm pressure. In order to assess the effect of usage of an implicit solvent model on the obtained relative energies single point calculations were carried out at the obtained geometries with the 6-311 + G(d) basis set and the solvation free energies were determined using the Polarizable Continuum Model (PCM) using the integral equation formalism variant (IEFPCM),¹⁷ the CPCM polarizable conductor calculation model,¹⁸ and the SMD solvent model.¹⁹ In all cases water was used as solvent. Furthermore, single point calculations were carried out at all stationary points using the B3LYP functional and all three continuum solvation models using the 6-311 + G(d) basis set.

The ionization constant of acids (K_a) is directly related to the Gibbs Free Energy change (ΔG) of the following reaction:



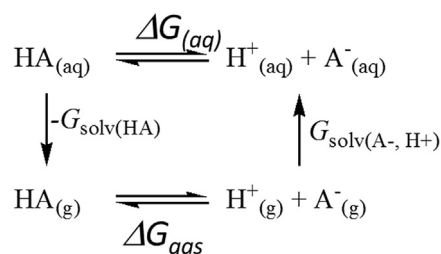
$$\Delta G_{(aq)} = -RT \ln K_a \quad (1)$$

where R is the universal gas constant and T is the temperature in K. From the rearrangement of this equation, and conversion of the natural logarithm to the ten-based logarithm, the pK_a value of the acids can be obtained.

$$pK_a = \frac{-\Delta G^*_{1ge}}{RT} \quad (2)$$

Thus in the present work we determined the Gibbs Free energies of HA(aq) and A⁻(aq) in solution from the DFT calculations. The free energy of the proton in gas phase was taken as -6.28 kcal/mol²⁰ and the hydration free energy of the proton was taken as -264.0 kcal/mol,²¹ although these value have been a question of much debate. It is worth noting that changing the value of these constants causes a systematic shift in the predicted pK_a value but it is not expected to change the observed trends in the pK_a values.

Using Hess's law the Gibbs free energy change of the ionization reaction can be divided into three parts as shown in Scheme 8.



Scheme 8. Thermodynamic cycle used to divide the overall Gibbs Free energy change of the ionization reaction to three components (Gas phase Gibbs Free Energy change, and solvation free energies).

$$\Delta G_{(aq)} = -G_{solv(HA)} + \Delta G_{gas} + G_{solv(H^+ + A^-)} \quad (3)$$

(2) molecular dynamics simulations

The lowest energy conformation of the neutral forms of **6** and **19** predicted by the conformational analysis were selected as starting structures for the molecular dynamics simulations. The structures were solvated in a cubic box of water and periodic boundary molecular dynamics simulations were run for 15 ns using Desmond²² and the OPLS_2005 force field.²³ The Ewald-summation was used to describe the coulomb interactions. The system was heated to 300 K using the Berendsen thermostat and then a 15 ns long MD simulation with a timestep of 2 fs was carried out in the NPT ensemble.

Acknowledgments

Financial supports of the National Research, Development and Innovation Office, NKFIH (earlier Hungarian Scientific Research Fund) (NKFIH/OTKA Grant No. 112289) and the New Széchenyi Development Plan (TÁMOP-4.2.1/B-09/1/KMR-2010-0002) are gratefully acknowledged. J.O. was supported by the Bolyai Janos Research Scholarship and by NKFIH/OTKA Grant No. 115503. This work was supported by the ÚNKP-16-3-III. New National Excellence Program of the Ministry of Human Capacities. The authors thank Dr. József Nagy and Prof. Jeremy Harvey for useful discussions.

Appendix A. Supplementary data

Supplementary data related to this article can be found at <http://dx.doi.org/10.1016/j.tet.2016.11.041>.

References

1. Steed JW, Atwood JL. *Supramolecular Chemistry*. second ed. Chichester, West Sussex, UK: Wiley; 2009.
2. Pedersen CJ. *J Am Chem Soc*. 1967;89:2495–2496.
3. (a) Izatt RM, Pawlak K, Bradshaw JS, Bruening RL. *Chem Rev*. 1995;95:2529–2586; (b) Zhang XX, Bradshaw JS, Izatt RM. *Chem Rev*. 1997;97:3313–3362;

- (c) Gokel GW, Leevy WM, Weber ME. *Chem Rev*. 2004;104:2723–2750;
- (d) Minkin VI. *Arkivoc*. 2008:90;
- (e) Bakó P, Rapi Zs, Keglevich Gy, et al. *Tetrahedron Lett*. 2011;52:1473–1476;
- (f) Newkome GR. *Prog Het Chem*. 2012;24:537–556;
- (g) Szabó T, Rapi Zs, Keglevich Gy, Szöllösy Á, Drahos L, Bakó P. *Arkivoc*. 2012;viii:36–48.
4. (a) Izatt RM, Lindh GC, Clark GA, et al. *J Membr Sci*. 1987;31:1–13; (b) Walkowiak W, Brown PR, Shukla JP, Bartsch RA. *J Membr Sci*. 1987;32:59–68; (c) Izatt RM, Lindh GC, Bruening RL, et al. *Anal Chem*. 1988;60:1694–1699; (d) Izatt RM, Lindh GC, Huszthy P, et al. *J Incl Phen Mol Rec Chem*. 1989;7:501–509; (e) Walkowiak W, Charewicz WA, Kang SI, Yang IW, Pugia MJ, Bartsch RA. *Anal Chem*. 1990;62:2018–2021; (f) Bradshaw JS. *J Incl Phen Mol Rec Chem*. 1997;29:221–246; (g) Bartsch RA, Jeon EG, Walkowiak W, Apostoluk W. *J Membr Sci*. 1999;159:123–131; (h) Huszthy P, Kertész J, Bradshaw JS, Izatt RM, Redd JT. *J Het Chem*. 2001;38:1259–1264; (i) Kovács I, Huszthy P, Bertha F, Sziebert D. *Tet Asym*. 2006;17:2538–2547; (j) Huszthy P, Farkas V, Tóth T, Székely Gy, Hollósi M. *Tetrahedron*. 2008;64:10107–10115; (k) Székely Gy, Farkas V, Párkányi L, Tóth T, Hollósi M, Huszthy P. *Struct Chem*. 2010;21:277–282; (l) Székely Gy, Csordás B, Farkas V, et al. *Eur J Org Chem*. 2012:3396–3407; (m) Szabó T, Hirsch E, Tóth T, Huszthy P. *Tet Asym*. 2014;25:1443–1449.
5. Szabó T, Hirsch E, Tóth T, et al. *Tet Asym*. 2015;26:650–656.
6. Mastryukova TA, Melent'eva TA, Shipov AE, Kabachnik MI. *Zhur Obsh Khim*. 1959;29:2178–2182.
7. Dhawan B, Redmore D. *J Org Chem*. 1986;51:179–183.
8. Watson DA, Chiu M, Bergman RG. *Organomet*. 2006;25:4731–4733.
9. <http://www.tomteoplastics.com/3dmg>.
10. Szegezdi J, Csizmadia F. 233rd ACS National Meeting CINF41, Chicago, USA, 2007; 2010. <http://www.chemaxon.com/product/pka.html>.
11. Riddick JA, Bunger WB, Sakano TK. *Organic Solvents: Physical Properties and Methods of Purification*. vol. 2. New York: Wiley-Interscience; 1986.
12. Tam KY, Takács-Novák K. *Anal Chim Acta*. 2001;434:157–167.
13. Völgyi G, Ruiz R, Box K, Comer J, Bosch E, Takács-Novák K. *Anal Chim Acta*. 2007;583:418–428.
14. Schrödinger. *Schrödinger Release 2015-2: MacroModel, Version 10.8*. NY: LLC; 2015.
15. Citation data can be obtained from here: http://gaussian.com/g_tech/g_ur/m_citation.htm (normal or reversed name order).
16. Zhao Y, Truhlar DG. *Theor Chem Acc*. 2007;120:215–241.
17. Tomasi J, Mennucci B, Cammi R. *Chem Rev*. 2005;105:2999–3093.
18. Barone V, Cossi M. *J Phys Chem A*. 1998;102:1995–2001.
19. Marenich AV, Cramer CJ, Truhlar DG. *J Phys Chem B*. 2009;113:6378–6396.
20. (a) Liptak MD, Shields GC. *J Am Chem Soc*. 2001;123:7314–7319; (b) Liptak MD, Gross KC, Seybold PG, Feldgus S, Shields GC. *J Am Chem Soc*. 2002;124:6421–6427.
21. Palasac MW, Shields GC. *J Phys Chem A*. 2004;108:3692–3694.
22. Schrödinger Release 2015-2: Desmond Molecular Dynamics System, version 4.2, D. E. Shaw Research, New York, NY, 2015. Maestro-Desmond Interoperability Tools, version 4.2, Schrödinger, New York, NY, 2015.
23. Banks JL, Beard HS, Cao Y, et al. *J Comp Chem*. 2005;26:1752–1780.